

Quadruply bonded complexes containing η^2 - or η^3 -tridentate phosphine ligands; syntheses, structures and $^{31}\text{P}\{^1\text{H}\}$ NMR spectra of $\text{Mo}_2\text{Cl}_4(\eta^3\text{-etp})(\text{L})$ and $\text{Mo}_2\text{Cl}_4(\eta^2\text{-etp})_2$ ($\text{L} = \text{CH}_3\text{OH}$, PMe_3 and PEt_3 ; $\text{etp} = \text{Ph}_2\text{PCH}_2\text{CH}_2\text{P}(\text{Ph})\text{CH}_2\text{CH}_2\text{PPh}_2$)

Chang-Tai Lee ^a, Wen-Kuei Yang ^a, Jhy-Der Chen ^{a,*}, Lin-Shu Liou ^b, Ju-Chun Wang ^b

^a Department of Chemistry, Chung-Yuan Christian University, Chung-Li, Taiwan, Republic of China

^b Department of Chemistry, Soochow University, Taipei, Taiwan, Republic of China

Received 21 March 1997; revised 4 June 1997; accepted 18 July 1997

Abstract

The reactive complex $\text{Mo}_2\text{Cl}_4(\eta^3\text{-etp})(\text{CH}_3\text{OH})$ ($\text{etp} = \text{Ph}_2\text{PCH}_2\text{CH}_2\text{P}(\text{Ph})\text{CH}_2\text{CH}_2\text{PPh}_2$) (**1**) was synthesized by reacting $(\text{NH}_4)_5\text{Mo}_2\text{Cl}_9$ with 1 equiv. of **etp** in CH_3OH . Reactions of **1** with PMe_3 and PEt_3 in THF gave $\text{Mo}_2\text{Cl}_4(\eta^3\text{-etp})(\text{PMe}_3)$ (**2**) and $\text{Mo}_2\text{Cl}_4(\eta^3\text{-etp})(\text{PEt}_3)$ (**3**) respectively. The complex $\alpha\text{-Mo}_2\text{Cl}_4(\eta^2\text{-etp})_2$ (**4**) was synthesized by refluxing $\text{Mo}_2\text{Cl}_4(\eta^3\text{-etp})(\text{CH}_3\text{OH})$ with 1 equiv. of **etp** in CH_3OH , where $\eta^3\text{-etp}$ is transformed to $\eta^2\text{-etp}$. Complex **4** can also be prepared by reacting $(\text{NH}_4)_5\text{Mo}_2\text{Cl}_9$ with 2 equiv. of **etp** in refluxing CH_3OH . Their UV-Vis and ^{31}P NMR spectra were recorded and the structures of **3** and **4** were determined. Crystal data for **3**: $\text{C}_{27}\text{H}_{34}$; space group $P2_1/n$, $a = 11.846(2)$, $b = 29.349(3)$, $c = 15.429(3)$ Å, $\beta = 112.52(1)^\circ$, $V = 4955(2)$ Å³, $Z = 4$, with final residuals $R = 0.0797$ and $R_w = 0.0811$. Crystal data for **4**: $\text{C}_{27}\text{H}_{34}$; space group $P2_1/c$, $a = 14.555(2)$, $b = 14.988(2)$, $c = 20.220(3)$ Å, $\beta = 106.80(1)^\circ$, $V = 4222(1)$ Å³, $Z = 2$, with final residuals $R = 0.0882$ and $R_w = 0.0893$. The **etp** ligands in **1–3** are coordinated to the Mo centers in tridentate fashion with chelating/bridging bonding modes. The **etp** ligands in **4** are chelated to the Mo centers in bidentate fashion through the central phosphorus atom and one terminal phosphorus atom. Complex **4** appears to be the first binuclear biligate complex chelated by linear tridentate ligands. Study of the $^{31}\text{P}\{^1\text{H}\}$ NMR spectrum of **3** leads to the conclusion that the through metal-metal quadruple bonding coupling $|^1J_{\text{P-Mo-Mo-P}}|$ is in the range from 18.18 to 24.28 Hz for complexes of the type $\text{Mo}_2\text{Cl}_4(\eta^3\text{-etp})(\text{L})$ ($\text{L} = \text{monodentate ligand}$). © 1998 Elsevier Science S.A. All rights reserved.

Keywords: Crystal structures; Molybdenum complexes; Quadruply bonded complexes; Tridentate phosphine complexes

1. Introduction

Quadruply bonded, dinuclear complexes containing tridentate or tetradentate phosphine ligands have been extensively studied during the last few years [1–4]. Complexes that have been structurally characterized include *rac*- Mo_2X_4 (tetraphos-1), *meso*- Mo_2X_4 (tetraphos-1) ($\text{X} = \text{Cl}$, Br ; tetraphos-1 = $\text{Ph}_2\text{PCH}_2\text{CH}_2\text{P}(\text{Ph})\text{CH}_2\text{CH}_2\text{P}(\text{Ph})\text{CH}_2\text{CH}_2\text{PPh}_2$) [2] and the mixed-phosphine complex $\text{Mo}_2\text{Cl}_4(\text{PEt}_3)(\eta^3\text{-tetraphos-2})$ (tetraphos-2 = $\text{P}(\text{CH}_2\text{CH}_2\text{PPh}_2)_3$) [3]. Recently, complexes containing both the bridging acetate ligand and polydentate phosphine ligand $\text{Mo}_2(\text{OAc})\text{Cl}_3(\eta^3\text{-etp})$ ($\text{etp} = \text{Ph}_2\text{PCH}_2\text{CH}_2\text{P}(\text{Ph})\text{CH}_2\text{CH}_2\text{PPh}_2$) and $\text{Mo}_2(\text{OAc})\text{Cl}_3(\eta^3\text{-tetraphos-2})$ were reported [4]. While the tetraphos-1 ligands are coordinated to the Mo cen-

ters to form bischelating/single-bridging bonding modes, the tetraphos-2 and the tridentate **etp** ligands are coordinated to the metal centers in tridentate fashion to form single-chelating/single-bridging bonding modes. $^{31}\text{P}\{^1\text{H}\}$ NMR spectra were applied to study the chemical shifts and $^{31}\text{P}\text{-}^{31}\text{P}$ couplings [3,4]. The through metal-metal quadruple bond coupling $|^3J_{\text{P-Mo-Mo-P}}|$ for the complexes $\text{Mo}_2(\text{OAc})\text{Cl}_3(\eta^3\text{-etp})$ and $\text{Mo}_2(\text{OAc})\text{Cl}_3(\eta^3\text{-tetraphos-2})$ was proposed to be 20 ± 1 Hz [4].

To study the potential reactivity of the quadruply bonded complex containing an η^3 -phosphine ligand, we have synthesized and studied the complex $\text{Mo}_2\text{Cl}_4(\eta^3\text{-etp})(\text{CH}_3\text{OH})$ in which the methanol ligand is weakly coordinated. This reactive compound provides a facile route for preparing several mixed-phosphine complexes of the type $\text{Mo}_2\text{Cl}_4(\eta^3\text{-etp})(\text{L})$ ($\text{L} = \text{PMe}_3$ or PEt_3) and a new type of binuclear biligate complex $\alpha\text{-Mo}_2\text{Cl}_4(\eta^2\text{-etp})_2$ which is chelated by linear tri-

* Corresponding author. Fax: +886-3-456 3160.

dentate ligands. The syntheses and structures of these complexes form the subject of this report. The $^{31}\text{P}\{^1\text{H}\}$ NMR spectra and the through metal–metal quadruple bond coupling constants of complexes of the type $\text{Mo}_2\text{Cl}_4(\eta^3\text{-etp})(\text{L})$ are also discussed.

2. Experimental

2.1. General procedures

All manipulations were carried out under dry, oxygen-free nitrogen using Schlenk techniques or a nitrogen box, unless otherwise noted. Solvents were dried and deoxygenated by refluxing over the appropriate reagents before use. Methanol was purified by distillation from magnesium, *n*-hexane, THF, benzene and toluene from sodium/benzophenone, and dichloromethane from P_2O_5 . The visible absorption spectra in dichloromethane were recorded on a Hitachi U-2000 spectrophotometer. The $^{31}\text{P}\{^1\text{H}\}$ NMR spectra were recorded on a Bruker 200 MHz NMR spectrometer. The $^{31}\text{P}\{^1\text{H}\}$ NMR chemical shift values were referenced externally and are reported relative to 85% H_3PO_4 . Elemental analyses were performed with a Perkin-Elmer 2400 elemental analyzer.

2.2. Starting materials

The complex $(\text{NH}_4)_5\text{Mo}_2\text{Cl}_9$ was prepared according to a previously published procedure [5]. The reagents bis-(2-diphenylphosphinoethyl)phenylphosphine (etp), PMe_3 (1 M in THF) and PEt_3 (1 M in THF) were purchased from Strem Chemical Co.

2.3. Preparation of $\text{Mo}_2\text{Cl}_4(\eta^3\text{-etp})(\text{CH}_3\text{OH})$

$(\text{NH}_4)_5\text{Mo}_2\text{Cl}_9$ (0.20 g, 0.32 mmol) and etp (0.172 g, 5.32 mmol) were placed in a flask containing 10 ml CH_3OH . The mixture was then stirred at room temperature for 3 h to yield a green solution and a green precipitate. The solid was filtered and washed with CH_3OH and then dried under reduced pressure. Yield 0.082 g (56%). UV–Vis (CH_3OH): 663 nm. *Anal. Calc.* for $\text{C}_{35}\text{H}_{37}\text{Cl}_4\text{OP}_3\text{Mo}_2$ (MW = 901.89): C, 46.57; H, 4.13. Found: C, 46.15; H, 3.95%. $^{31}\text{P}\{^1\text{H}\}$ NMR ($\text{CDCl}_3/\text{CH}_2\text{Cl}_2$): 24.40 (dd), 39.18 (dd), 44.16 (dd) ppm.

2.4. Preparations of $\text{Mo}_2\text{Cl}_4(\eta^3\text{-etp})(\text{PMe}_3)$ and $\text{Mo}_2\text{Cl}_4(\eta^3\text{-etp})(\text{PEt}_3)$

$\text{Mo}_2\text{Cl}_4(\text{etp})(\text{CH}_3\text{OH})$ (0.10 g, 0.10 mmol) was placed in a flask containing 10 ml THF. 1 M PMe_3 or PEt_3 in THF (0.10 ml, 0.10 mmol) was then added to the flask dropwise. The mixture was stirred at room temperature for 30 min. The volume of the solution was then reduced and 20 ml of *n*-hexane added to induce precipitation. The green solid was filtered and dried under reduced pressure. Results for $\text{Mo}_2\text{Cl}_4(\eta^3\text{-etp})(\text{PMe}_3)$. Yield 0.051 g (53%). UV–Vis

(THF): 655, 452 nm. *Anal. Calc.* for $\text{C}_{37}\text{H}_{42}\text{Cl}_4\text{P}_3\text{Mo}_2$ (MW = 945.91): C, 46.94; H, 4.47. Found: C, 46.19; H, 4.40%. Results for $\text{Mo}_2\text{Cl}_4(\eta^3\text{-etp})(\text{PEt}_3)$. Yield 0.049 g (52%). UV–Vis (THF): 661, 468 nm. *Anal. Calc.* for $\text{C}_{40}\text{H}_{48}\text{Cl}_4\text{P}_3\text{Mo}_2$ (MW = 987.96): C, 48.59; H, 4.90. Found: C, 48.45; H, 4.75%.

2.5. Preparation of $\alpha\text{-Mo}_2\text{Cl}_4(\eta^2\text{-etp})_2$

(A) $\text{Mo}_2\text{Cl}_4(\text{etp})(\text{CH}_3\text{OH})$ (0.023 g, 0.025 mmol) was placed in a flask containing 7 ml CH_3OH . The ligand etp (0.014 g, 0.025 mmol) was then added. The mixture was allowed to reflux for 24 h to yield a green solution and green precipitate. The solid was filtered and washed with CH_3OH and then dried under reduced pressure. Yield 0.0056 g (25%). UV–Vis spectrum in CH_2Cl_2 : 677 nm. $^{31}\text{P}\{^1\text{H}\}$ NMR ($\text{CDCl}_3/\text{CH}_2\text{Cl}_2$): –12.55 (d), 44.39 (dd), 49.64 (m) ppm. *Anal. Calc.* for $\text{C}_{68}\text{H}_{66}\text{Cl}_4\text{P}_6\text{Mo}_2$ (MW = 1404.05): C, 58.12; H, 4.74. Found: C, 57.44; H, 4.74%. (B) $(\text{NH}_4)_5\text{Mo}_2\text{Cl}_9$ (0.051 g, 0.080 mmol) and etp (0.086 g, 0.16 mmol) were placed in a flask containing 7 ml CH_3OH . The mixture was then refluxed at room temperature for 24 h to yield a green solution and green precipitate. The solid was filtered and washed with CH_3OH and then dried under reduced pressure. Yield 0.035 g (51%). UV–Vis and NMR spectra are the same as those for the compound obtained in (A).

3. X-ray crystallography

3.1. $\text{Mo}_2\text{Cl}_4(\eta^3\text{-etp})(\text{PEt}_3)\cdot\text{C}_6\text{H}_6$

The diffraction data of $\text{Mo}_2\text{Cl}_4(\eta^3\text{-etp})(\text{PEt}_3)$ were collected on a Siemens P4 diffractometer, which was equipped with graphite-monochromated $\text{Mo K}\alpha$ ($\lambda_{\text{Cu}} = 0.71037 \text{ \AA}$) radiation. Data reduction was carried out by standard methods with the use of well established computational procedures [6]. Crystals of $\text{Mo}_2\text{Cl}_4(\eta^3\text{-etp})(\text{PEt}_3)$ suitable for X-ray diffraction measurement were obtained by hexane-induced crystallization from a toluene solution.

A green crystal of $\text{Mo}_2\text{Cl}_4(\eta^3\text{-etp})(\text{PEt}_3)$ was mounted on the top of a glass fiber with epoxy cement. The unit cell constants were determined from 25 reflections with 2θ in the range from 12 to 25°. These were consistent with the monoclinic crystal system, and the space group was subsequently determined to be $P2_1/n$. Routine ω data collection was used to scan the data points in the range $3^\circ < 2\theta < 50^\circ$. The structure factors were obtained after Lorentz and polarization corrections. Empirical absorptions based on azimuthal (Ψ) scans of reflections of Eulerian angles χ near 90° were applied to the data. The programs in SHELXTL PLUS were used to solve the structure, which led to the location of the positions of several heavier atoms. The remaining atoms were found in a series of alternating difference Fourier maps and least-

Table 1
Crystal data for $3 \cdot C_7H_8$ and $4 \cdot 2C_7H_8$

Complex	$3 \cdot C_7H_8$	$4 \cdot 2C_7H_8$
Formula	$Mo_2P_2Cl_4C_{14}H_{28}$	$Mo_2P_2Cl_4C_{28}H_{56}$
FW	1078.55	1587.04
Space group	$P2_1/n$	$P2_1/c$
a (Å)	11.846(2)	14.555(2)
b (Å)	29.349(3)	14.988(2)
c (Å)	15.429(3)	20.220(3)
β (°)	112.52(1)	106.80(1)
V (Å ³)	4955(2)	4222(1)
Z	4	2
d_{calc} (g cm ⁻³)	1.446	1.248
Crystal size (mm)	0.3 × 0.2 × 0.1	0.2 × 0.2 × 0.1
μ (Mo K α) (mm ⁻¹)	0.882	0.576
Data collection instrument	Siemens P4	Siemens P4
Radiation monochromated in incident beam (Mo K α) (Å)	0.71073	0.71073
No. orientation reflections: range 2θ (°)	25: $12 < 2\theta < 25$	25: $18.5 < 2\theta < 20$
Temperature (°C)	25	25
Scan method	ω	ω
Data collection range (2θ) (°)	$3 < 2\theta < 50$	$3 < 2\theta < 50$
No. unique data	8688	7424
No. observed data	3557	1278
Criterion for observed data	$F > 4\sigma(F)$	$F > 5\sigma(F)$
No. parameters refined	480	222
R^a	0.0797	0.0882
R_w^b	0.0811	0.0893
Quality-of-fit indicator ^c	1.34	1.47
Largest shift/e.s.d., final cycle	0.002	0.000
Largest peak (e Å ⁻³)	0.92	0.79

$$^a R = \sum ||F_o| - |F_c|| / \sum |F_o|$$

$$^b R_w = [\sum w(|F_o| - |F_c|)^2 / \sum w|F_o|^2]^{1/2}, w = 1/[\sigma^2(F_o) + gF_o^2]$$

$$^c \text{Quality-of-fit} = [\sum w(|F_o| - |F_c|)^2 / (N_{observed} - N_{parameters})]^{1/2}$$

square refinements. The C(5) atom was found to be disordered and the occupancies of the two carbon atoms were set to be 0.5. The final residuals of the refinement were $R = 0.0797$ and $R_w = 0.0811$. Basic information pertaining to crystal parameters and structure refinement is summarized in Table 1. Tables 2 and 3 list positional parameters and selected bond distances and angles respectively.

3.2. $\alpha\text{-Mo}_2Cl_4(\eta^2\text{-etp})_2 \cdot 2C_7H_8$

The crystallographic procedures for determining the structure of $\alpha\text{-Mo}_2Cl_4(\eta^2\text{-etp})_2$ were similar to those for complex **3**. Crystals of $\alpha\text{-Mo}_2Cl_4(\eta^2\text{-etp})_2$ suitable for X-ray diffraction measurement were obtained by hexane-induced crystallization from a toluene–benzene solution. The crystals conformed to the space group $P2_1/c$. The final residuals of the refinement were $R = 0.0882$ and $R_w = 0.0893$. Basic information pertaining to crystal parameters and structure refinement is summarized in Table 1. Tables 4 and 5 list positional parameters and selected bond distances and angles respectively.

4. Results and discussion

4.1. Syntheses and absorption spectra

The reactive complex $Mo_2Cl_4(\eta^3\text{-etp})(CH_3OH)$ (**1**) was synthesized by reacting $(NH_4)_5Mo_2Cl_{10}$ with 1 equiv. of etp

Table 2
Atomic coordinates and equivalent isotropic displacement coefficients (Å²) for **3**

	x	y	z	U_{eq}
Mo(1)	0.5507(1)	0.1438(1)	0.4405(1)	0.039(1)
Mo(2)	0.5843(1)	0.2109(1)	0.3985(1)	0.044(1)
Cl(1)	0.5803(4)	0.0838(2)	0.3438(3)	0.061(2)
Cl(2)	0.3313(4)	0.1344(2)	0.3611(3)	0.061(2)
Cl(3)	0.4024(4)	0.2379(2)	0.2767(3)	0.067(2)
Cl(4)	0.7868(4)	0.2373(2)	0.4878(3)	0.065(2)
P(1)	0.5214(4)	0.2675(2)	0.4992(3)	0.049(2)
P(2)	0.5466(4)	0.1577(2)	0.6027(3)	0.044(2)
P(3)	0.7628(4)	0.1209(2)	0.5503(3)	0.044(2)
P(4)	0.6490(7)	0.1952(2)	0.2612(4)	0.089(3)
C(1)	0.803(1)	0.156(1)	0.655(1)	0.04(1)
C(2)	0.705(1)	0.152(1)	0.693(1)	0.05(1)
C(3)	0.502(1)	0.212(1)	0.640(1)	0.05(1)
C(4)	0.567(2)	0.255(1)	0.622(1)	0.06(1)
C(5A)	0.479(6)	0.161(2)	0.161(4)	0.08(3)
C(5B)	0.590(5)	0.155(2)	0.172(3)	0.10(3)
C(6)	0.493(4)	0.158(1)	0.094(3)	0.22(3)
C(7)	0.646(2)	0.247(1)	0.198(2)	0.11(1)
C(8)	0.730(2)	0.286(1)	0.261(2)	0.13(2)
C(9)	0.804(2)	0.173(1)	0.296(2)	0.15(2)
C(10)	0.870(2)	0.173(1)	0.233(2)	0.16(2)
C(11)	0.893(2)	0.118(1)	0.517(1)	0.05(1)
C(12)	0.900(2)	0.081(1)	0.461(1)	0.08(1)
C(13)	0.997(3)	0.078(1)	0.433(2)	0.11(2)
C(14)	1.087(2)	0.111(1)	0.457(2)	0.12(2)

(continued)

Table 2 (continued)

	x	y	z	U_{eq}
C(15)	1.082(2)	0.146(1)	0.514(2)	0.09(1)
C(16)	0.988(2)	0.149(1)	0.543(1)	0.07(1)
C(21)	0.763(2)	0.063(1)	0.600(1)	0.05(1)
C(22)	0.877(2)	0.046(1)	0.664(1)	0.08(1)
C(23)	0.882(3)	0.005(1)	0.709(2)	0.10(1)
C(24)	0.780(3)	-0.019(1)	0.691(2)	0.10(2)
C(25)	0.669(2)	-0.004(1)	0.624(1)	0.09(1)
C(26)	0.665(2)	0.038(2)	0.579(1)	0.06(1)
C(31)	0.459(2)	0.117(1)	0.640(1)	0.05(1)
C(32)	0.457(2)	0.119(1)	0.727(2)	0.10(1)
C(33)	0.390(3)	0.089(1)	0.757(2)	0.14(2)
C(34)	0.328(3)	0.056(1)	0.701(2)	0.13(2)
C(35)	0.332(2)	0.051(1)	0.615(2)	0.09(1)
C(36)	0.393(2)	0.083(1)	0.582(2)	0.09(1)
C(41)	0.360(1)	0.280(1)	0.465(1)	0.05(1)
C(42)	0.274(2)	0.245(1)	0.432(1)	0.06(1)
C(43)	0.150(2)	0.255(1)	0.411(1)	0.08(1)
C(44)	0.109(2)	0.296(1)	0.422(2)	0.09(1)
C(45)	0.196(2)	0.330(1)	0.456(2)	0.08(1)
C(46)	0.320(2)	0.324(1)	0.477(1)	0.06(1)
C(51)	0.589(2)	0.324(1)	0.497(1)	0.05(1)
C(52)	0.566(2)	0.343(1)	0.414(2)	0.09(1)
C(53)	0.613(3)	0.386(1)	0.409(2)	0.14(2)
C(54)	0.680(3)	0.409(1)	0.490(2)	0.12(2)
C(55)	0.708(2)	0.389(1)	0.573(2)	0.10(1)
C(56)	0.659(2)	0.347(1)	0.580(1)	0.08(1)

Equivalent isotropic U defined as one-third of the trace of the orthogonalized U_{ij} tensor.

Table 3

Selected bond distances (Å) and angles (°) for 3

Distances			
Mo(1)=Mo(2)	2.159(2)	Mo(1)-Cl(1)	2.418(5)
Mo(1)=Cl(2)	2.427(4)	Mo(1)-P(2)	2.555(5)
Mo(1)=P(3)	2.525(4)	Mo(2)-Cl(3)	2.387(4)
Mo(2)=Cl(4)	2.391(4)	Mo(2)-P(1)	2.571(6)
Mo(2)=P(4)	2.556(8)		
Angles			
Mo(2)=Mo(1)-Cl(1)	113.1(2)	Mo(2)=Mo(1)-Cl(2)	103.7(1)
Cl(1)=Mo(1)-Cl(2)	89.3(2)	Mo(2)=Mo(1)-P(2)	102.8(1)
Cl(1)=Mo(1)-P(2)	141.6(2)	Cl(2)=Mo(1)-P(2)	95.4(2)
Mo(2)=Mo(1)-P(3)	101.1(1)	Cl(1)=Mo(1)-P(3)	83.0(2)
Cl(2)=Mo(1)-P(3)	155.1(2)	P(2)=Mo(1)-P(3)	76.8(2)
Mo(1)=Mo(2)-Cl(3)	108.9(1)	Mo(1)=Mo(2)-Cl(4)	112.5(1)
Cl(3)=Mo(2)-Cl(4)	138.6(2)	Mo(1)=Mo(2)-P(1)	106.1(1)
Cl(3)=Mo(2)-P(1)	83.1(2)	Cl(4)=Mo(2)-P(1)	84.4(2)
Mo(1)=Mo(2)-P(4)	103.4(2)	Cl(3)=Mo(2)-P(4)	82.7(2)
Cl(4)=Mo(2)-P(4)	89.0(2)	P(1)=Mo(2)-P(4)	150.0(2)

in CH₃OH at room temperature. Reactions of **1** with PMe₃ and PEt₃ in THF gave the complexes Mo₂Cl₄(η³-etp)(PMe₃) (**2**) and Mo₂Cl₄(η³-etp)(PEt₃) (**3**) respectively. On the basis of the results of elemental analyses, UV-Vis and ³¹P{¹H} NMR spectra, the structures of **1** and **2** are presumably similar to that of **3** discussed below. It is clearly shown that complex **1** is a convenient starting material for making mixed-ligand complexes of the type Mo₂Cl₄(η³-etp)(L) (L = monodentate ligand). The absorption spectra for **1**–**3**

Table 4

Atomic coordinates and equivalent isotropic displacement coefficients (Å²) for 4

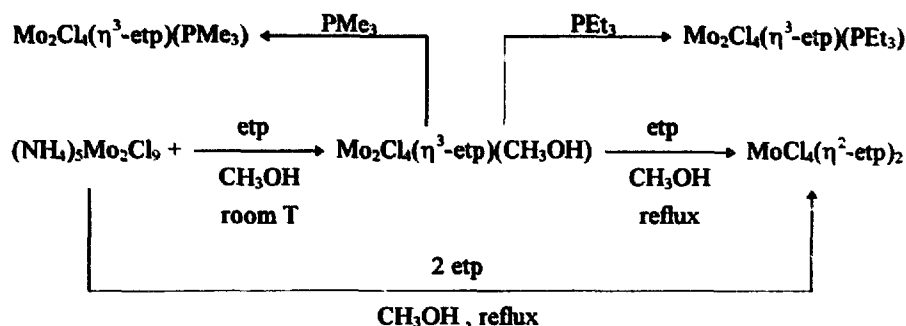
	x	y	z	U_{eq}
Mo(1)	0.0070(2)	0.5085(2)	0.054(1)	0.042(1)
Cl(1)	0.0950(7)	0.3877(6)	0.1235(5)	0.064(5)
Cl(2)	0.1406(7)	0.6061(7)	0.1105(5)	0.072(5)
P(1)	-0.1134(7)	0.6323(6)	0.0439(5)	0.049(5)
P(2)	-0.1434(7)	0.4302(6)	0.0625(5)	0.052(5)
P(3)	-0.2781(8)	0.1621(7)	0.0007(6)	0.081(6)
C(1)	-0.232(2)	0.588(2)	-0.001(2)	0.06(1)
C(2)	-0.251(2)	0.487(2)	0.009(1)	0.05(1)
C(3)	-0.160(2)	0.310(2)	0.039(2)	0.06(1)
C(4)	-0.269(3)	0.281(2)	0.027(2)	0.09(1)
C(11)	-0.110(3)	0.743(2)	0.002(2)	0.07(1)
C(12)	-0.186(3)	0.782(3)	-0.044(2)	0.09(1)
C(13)	-0.164(3)	0.862(3)	-0.074(2)	0.09(1)
C(14)	-0.079(3)	0.901(3)	-0.052(2)	0.08(1)
C(15)	-0.009(3)	0.867(2)	-0.007(2)	0.08(1)
C(16)	-0.017(3)	0.784(3)	0.028(2)	0.09(1)
C(21)	-0.121(2)	0.666(2)	0.129(2)	0.05(1)
C(22)	-0.202(3)	0.716(2)	0.131(2)	0.10(1)
C(23)	-0.203(3)	0.743(3)	0.200(2)	0.11(2)
C(24)	-0.138(3)	0.714(2)	0.256(2)	0.07(1)
C(25)	-0.061(3)	0.660(2)	0.255(2)	0.07(1)
C(26)	-0.053(3)	0.631(2)	0.191(2)	0.07(1)
C(31)	-0.156(2)	0.427(2)	0.148(2)	0.04(1)
C(32)	-0.226(2)	0.473(2)	0.169(2)	0.06(1)
C(33)	-0.233(3)	0.469(2)	0.235(2)	0.10(1)
C(34)	-0.170(3)	0.417(2)	0.281(2)	0.08(1)
C(35)	-0.104(3)	0.366(2)	0.265(2)	0.07(1)
C(36)	-0.100(3)	0.376(2)	0.199(2)	0.07(1)
C(41)	-0.223(2)	0.102(2)	0.083(2)	0.05(1)
C(42)	-0.222(3)	0.127(3)	0.149(2)	0.11(1)
C(43)	-0.181(3)	0.067(3)	0.205(2)	0.13(2)
C(44)	-0.148(3)	-0.010(3)	0.190(2)	0.11(1)
C(45)	-0.142(3)	-0.038(3)	0.131(2)	0.10(2)
C(46)	-0.181(2)	0.016(3)	0.077(2)	0.08(1)
C(51)	-0.412(4)	0.144(3)	-0.008(3)	0.12(1)
C(52)	-0.466(6)	0.123(4)	-0.075(5)	0.29(4)
C(53)	-0.567(7)	0.121(5)	-0.083(5)	0.30(5)
C(54)	-0.585(5)	0.114(4)	-0.039(4)	0.18(3)
C(55)	-0.567(5)	0.140(4)	0.022(4)	0.22(3)
C(56)	-0.453(5)	0.149(4)	0.038(3)	0.21(3)

Equivalent isotropic U defined as one-third of the trace of the orthogonalized U_{ij} tensor.

Table 5

Selected bond distances (Å) and angles (°) for 4

Bond distances			
Mo(1)-Cl(1)	2.419(9)	Mo(1)-Cl(2)	2.438(10)
Mo(1)-P(1)	2.519(10)	Mo(1)-P(2)	2.533(11)
Mo(1)-Mo(1A)	2.149(6)		
Bond angles			
Cl(1)-Mo(1)-Cl(2)	87.7(3)	Cl(1)-Mo(1)-P(1)	146.9(4)
Cl(2)-Mo(1)-P(1)	92.2(3)	Cl(1)-Mo(1)-P(2)	86.4(3)
Cl(2)-Mo(1)-P(2)	146.5(4)	P(1)-Mo(1)-P(2)	75.7(3)
Cl(1)-Mo(1)-Mo(1A)	112.3(3)	Cl(2)-Mo(1)-Mo(1A)	112.1(3)
P(1)-Mo(1)-Mo(1A)	98.4(3)	P(2)-Mo(1)-Mo(1A)	100.6(3)



are typical for complexes containing metal–metal quadruple bonds. The lowest energy bands which appear at 663 (CH₃OH), 655 (THF) and 661 (THF) nm can be assigned to $\delta \rightarrow \delta^*$ transitions [1] for complexes 1, 2 and 3 respectively.

The reaction of Mo₂Cl₄(η^3 -etp)(CH₃OH) with 1 equiv. of etp in refluxing CH₃OH produced the complex α -Mo₂Cl₄(η^2 -etp)₂ (4). Clearly, η^3 -etp in 1 is transformed to η^2 -etp by breaking one of the Mo–P bonds. Complex 4 can also be prepared by reacting (NH₄)₅Mo₂Cl₉ with 2 equiv. of etp in refluxing CH₃OH. The lowest absorption band of 4 at 664 nm in THF solvent (675 nm in CH₂Cl₂) can be assigned to $\delta \rightarrow \delta^*$ transitions. This value is similar to those of structurally characterized chelating complexes, i.e. 677 nm for α -Mo₂Cl₄(dppe)₂ [7], 675 nm for *anti*- α -Mo₂Cl₄(dpdt)₂ [8], and 669 nm for *anti*- α -Mo₂Cl₄(dpdbp)₂ [9]. The formation pathways for complexes 1–4 are shown in Scheme 1.

4.2. Molecular structure of Mo₂Cl₄(η^3 -etp)(PEt₃) 3

Green crystals of 3 conform to the space group $P2_1/n$ with four molecules in a unit cell. Fig. 1 shows the ORTEP diagram of 3. The etp ligand coordinates to the molybdenum atoms in a tridentate fashion and forms one chelating ring and one bridging ring with the Mo atoms, which are five- and six-membered respectively. The six-membered ring adopts the less sterically demanding boat configuration. The two phosphorus atoms which are coordinated to the same molybdenum atom are *cis* to each other owing to ligand constraints. This η^3 bonding mode of the etp ligand was seen in the quadruply bonded complex Mo₂(OAc)Cl₃(η^3 -etp) [4]. The central phosphorus atom of the achiral etp ligand becomes chiral upon coordination to the molybdenum atoms.

Fig. 2 shows a view of the inner part of 3 looking down the Mo–Mo bond. The Λ configuration formed by the four smallest torsional angles (average 12.2°) is found for 3. Since the complex crystallized in the centrosymmetric space group $P2_1/n$, it should have two molecules with Δ/R configuration and the other two with Λ/S configuration in a unit cell. The internal rotation angles of complexes 3, Mo₂Cl₄(PEt₃)(η^3 -tetrphos-2) [3], Mo₂(OAc)Cl₃(etp) [4] and Mo₂(OAc)Cl₃(tetrphos-2) [4] are listed in Table 6 for comparison. It is interesting that these molecules have a similar trend of

internal rotation angle, starting from the largest P–Mo–Mo–P angles to the smallest P–Mo–Mo–Cl or O–Mo–Mo–O angles. The twist angle of Cl–Mo–Mo–P in 3 is even smaller than those of O–Mo–Mo–O in Mo₂(OAc)Cl₃(etp) [4] and Mo₂(OAc)Cl₃(tetrphos-2) [4]. It is clearly shown again that the non-bonded steric repulsions resulting from the chelating/bridging bonding mode play a major role in determining the twist angle [4].

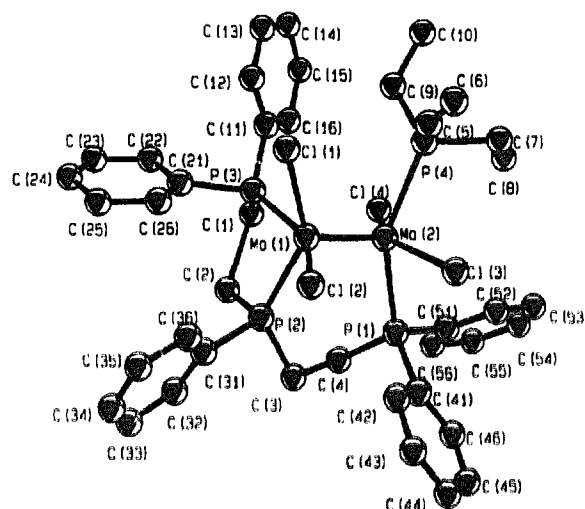


Fig. 1. ORTEP drawing of 3 in its entirety.

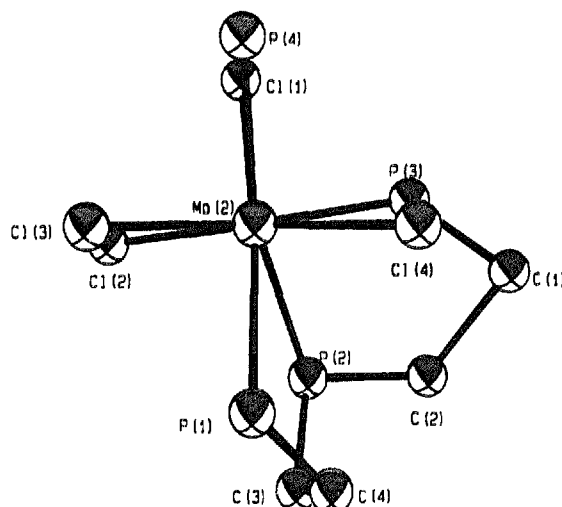


Fig. 2. View looking down the Mo–Mo bond for 3.

Table 6
Comparison of the internal rotation angles for compounds with η^1 -phosphine ligands

Complex	Mo–Mo (Å)	P–Mo–Mo–P	Cl–Mo–Mo–Cl	Cl–Mo–Mo–P	P(O)–Mo–Mo–Cl(O)	Average
3	2.159(2)	20.7	9.8	8.8	1.7	12.2
5	2.126(3)	22.1	11.0	13.9	6.2	13.2
6a	2.121(3)	18.7	8.8	11.2	7.0	11.4
6b	2.134(3)	–19.0	–9.8	–10.1	–6.7	–11.4
7	2.132(3)	19.4	12.5	10.0	4.7	11.7

Complex 5 = $\text{Mo}_2\text{Cl}_4(\text{OAc})(\eta^1\text{-tetraphos-2})$. Complex 6 = $\text{Mo}_2\text{Cl}_4(\text{OAc})(\eta^1\text{-etp})$. Complex 7 = $\text{Mo}_2\text{Cl}_4(\text{PEt}_3)(\eta^1\text{-tetraphos-2})$.

4.3. Molecular structure of $\alpha\text{-Mo}_2\text{Cl}_4(\eta^2\text{-etp})_2$ 4

The crystal of 4 conforms to the space group $P2_1/c$ with two molecules in a unit cell. Fig. 3 shows the ORTEP diagram of 4. The molecule is located in a crystallographically imposed inversion center. Each etp ligand chelates the Mo centers through the central phosphorus atom and one terminal phosphorus atom, and the other terminal phosphorus atom is not coordinated. The achiral central phosphorus atom of

the free phosphine ligands becomes chiral upon coordination to the molybdenum atoms. The Mo–Mo bond distance of 2.149(6) Å for 4 is similar to those observed in $\alpha\text{-Mo}_2\text{Cl}_4(\text{dppe})_2$ (2.140(2) Å) [7], *anti*- $\alpha\text{-Mo}_2\text{Cl}_4(\text{dpdt})_2$ (2.147(1) Å) [8], and *anti*- $\alpha\text{-Mo}_2\text{Cl}_4(\text{dpdbp})_2$ (2.149(1) Å) [9]. Fig. 4 shows a view of the inner part of 1 looking down the Mo–Mo bond. Although the Mo–L bonds of the halves of the dimer are not eclipsed, the average L–Mo–Mo–L twist angle is zero owing to symmetry requirement.

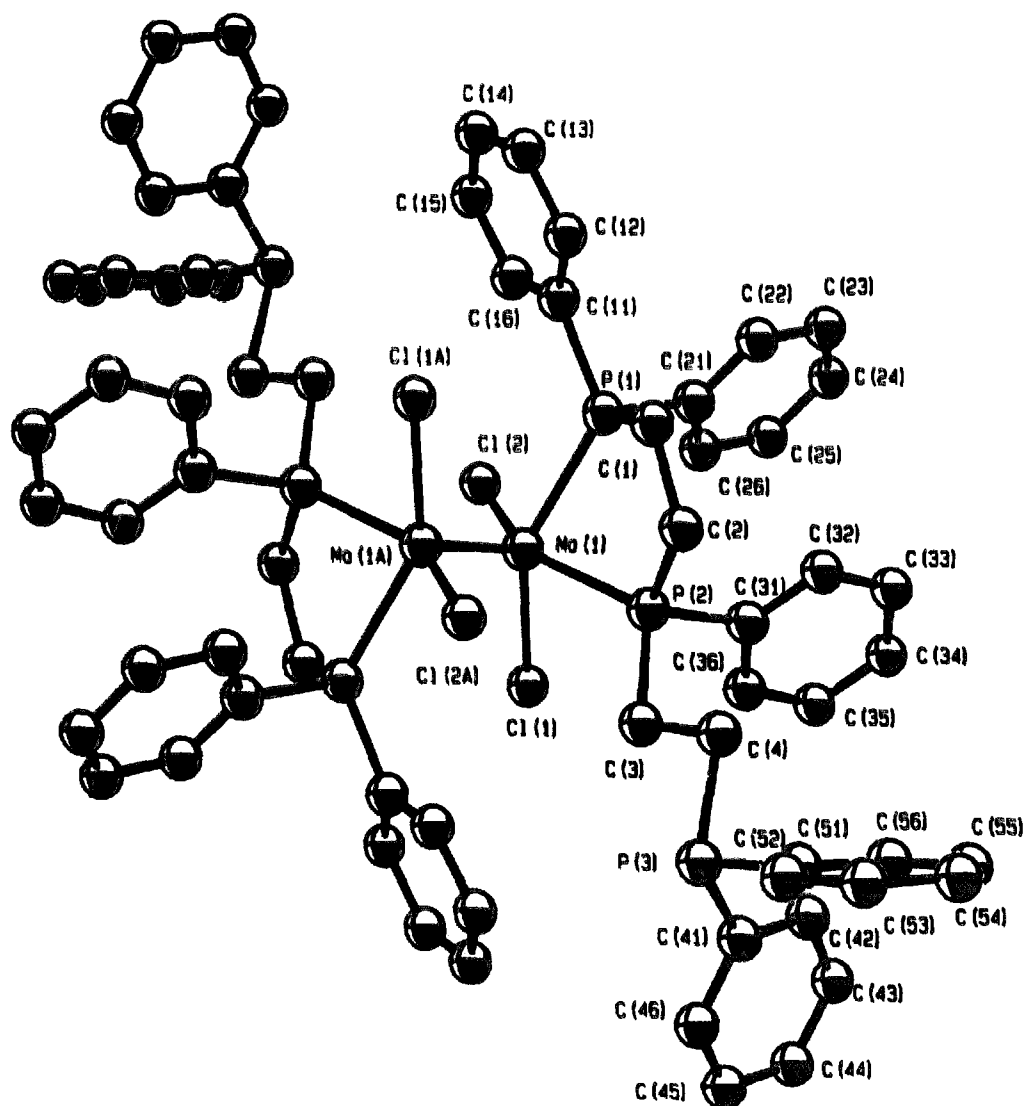


Fig. 3. ORTEP drawing of 4 in its entirety.

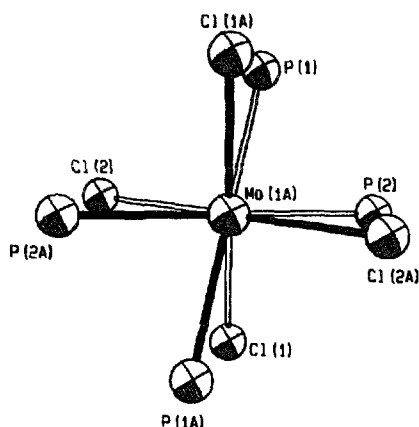


Fig. 4. View looking down the Mo–Mo bond for 4.

A number of coordination modes is possible for a given polydentate phosphine ligand, but in practice only some are observed [10,11]. For the dinuclear complexes containing linear tridentate phosphine ligands, only two types of bonding modes were observed [10]. In the first type, the tridentate phosphine ligand acts as both a chelating and bridging ligand, as seen in the singly bonded complex $\text{Rh}_2[(\mu\text{-dmmm})_2(\text{CO})_2]^+$ (dmmm = $\text{MeP}(\text{CH}_2\text{PMe}_2)_2$) [12], the triply bonded complex $[\text{Re}_2\text{Cl}_3(\text{dpmp})_2]^+$ (dpmp = $\text{PhP}(\text{CH}_2\text{-PPh}_2)_2$) [13], and the quadruply bonded complexes $\text{Mo}_2(\text{OAc})\text{Cl}_3(\eta^3\text{-etp})$ [4] and complexes 1–3. Complexes without metal–metal bonds, such as $\text{Pd}_2\text{Cl}_4(\text{NCMe})(\text{dpmp})$, have also been prepared [12]. The other type of complex is $[(\text{etp})\text{Fe}(\mu\text{-SH})_3\text{Fe}(\text{etp})](\text{ClO}_4)$, in which the tridentate ligand etp bischelates to the metal centers [14]. In all these complexes, the phosphine ligands coordinate to the metal centers in tridentate fashion and can be classified as binuclear triligate complexes [10]. Complex 4 is thus the first binuclear biligate complex chelated by linear tridentate ligands [10].

4.4. NMR spectra of 1–3

The $^{31}\text{P}\{^1\text{H}\}$ NMR spectra of complexes 2 and 3 (Fig. 5(b) and (d)) display four multiplets. All the peaks in complex 2 or 3 are coupled to each other. Comparison of the chemical shifts of complexes 2 and 3 clearly shows that the multiplet of 2 at -2.00 ppm and that of 3 at 16.59 ppm are dependent on the natures of the monodentate phosphine ligands, PMe_3 and PEt_3 respectively. These two multiplets can thus be assigned to PMe_3 and PEt_3 respectively, which are named as atoms P(4). Detailed analysis of the structures shows that atom P(4) can couple with two phosphorus atoms through only metal–metal quadruple bonds. These two coupling constants (i.e. $|^3J_{\text{P}(2)\text{-Mo-Mo-P}(4)}|$ and $|^3J_{\text{P}(3)\text{-Mo-Mo-P}(4)}|$) should be similar. Referring to the three coupling constants associated with atoms P(4), the peaks at 23.28 ppm for 2 and 23.99 ppm for 3 are assigned to atoms P(1) since $^2J_{\text{P}(1)\text{-Mo-P}(4)}$ is 147.22 Hz for 2 and 136.10 Hz for 3 respectively, and are much larger than $|^4J_{\text{P}(2)\text{-Mo-Mo-P}(4)}|$ and $|^3J_{\text{P}(3)\text{-Mo-Mo-P}(4)}|$. This assignment is consistent with the prediction that the coupling between the *trans* phosphorus

atoms on the same metal center will give the largest $J_{\text{P-P}}$ coupling constant, which has also been suggested for the complex $\text{Mo}_2\text{Cl}_4(\text{PEt}_3)(\eta^3\text{-tetraphos-2})$ [3]. We are now left with two peaks at 31.87 and 45.65 ppm in 2 and 30.62 and 44.78 in 3 for atoms P(2) and P(3). It is also clearly seen that atoms P(1) couple with atoms P(3) through only metal–metal quadruple bonds. The coupling constant $|^3J_{\text{P}(1)\text{-Mo-Mo-P}(3)}|$ should be similar to $|^3J_{\text{P}(2)\text{-Mo-Mo-P}(4)}|$ and $|^3J_{\text{P}(3)\text{-Mo-Mo-P}(4)}|$. Comparison of the coupling constants leads to the conclusion that the peaks at 45.65 ppm in 2 and 44.78 ppm in 3 belong to atoms P(3). Consequently, the peaks at 31.87 ppm in 2 and 30.62 ppm in 3 are assigned to atoms P(2). Spectrum simulations were done by employing the coupling constants listed in Tables 7 and 8, and produced the result shown in Fig. 5(a) and (c) for 2 and 3 respectively.

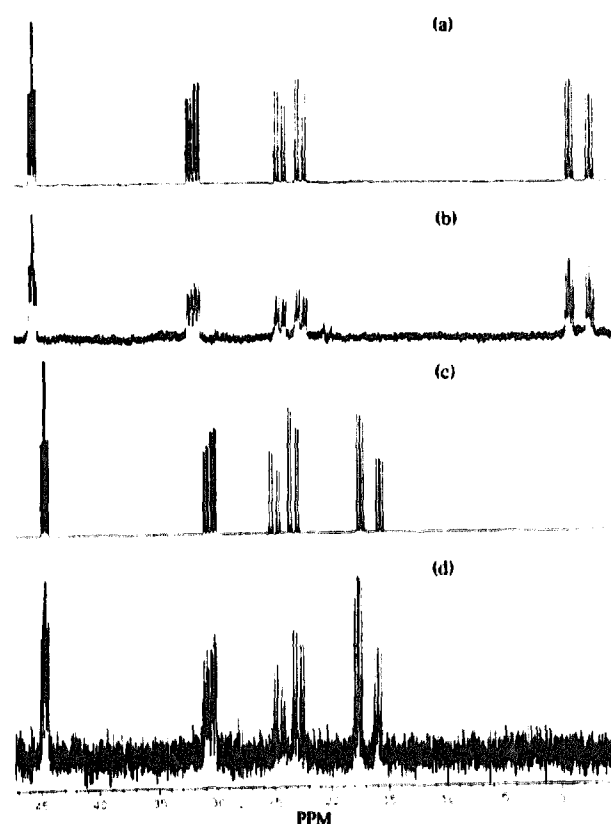


Fig. 5. (a) Simulation spectrum of 2. (b) $^{31}\text{P}\{^1\text{H}\}$ MR spectra of 2 in CDCl_3 . (c) Simulation spectrum of 3. (d) $^{31}\text{P}\{^1\text{H}\}$ NMR spectra of 3 in CDCl_3 .

Table 7
 $^{31}\text{P}\{^1\text{H}\}$ NMR data for $\text{Mo}_2\text{Cl}_4(\eta^3\text{-etp})(\text{PMe}_3)$

Nuclear	δ (ppm)	Coupling	Experimental value (Hz)
P(1)	23.28	P(1)–P(2)	51.24
P(2)	31.87	P(1)–P(3)	19.29
P(3)	45.65	P(1)–P(4)	147.22
P(4)	-2.00	P(2)–P(3)	7.73
		P(2)–P(4)	24.70
		P(3)–P(4)	19.15

Table 8
 $^{31}\text{P}\{^1\text{H}\}$ NMR data for $\text{Mo}_2\text{Cl}_4(\eta^1\text{-etp})(\text{PEt}_3)$

Nuclear	δ (ppm)	Coupling	Experimental value (Hz)
P(1)	23.99	P(1)–P(2)	52.05
P(2)	30.62	P(1)–P(3)	18.44
P(3)	44.78	P(1)–P(4)	136.10
P(4)	16.59	P(2)–P(3)	8.25
		P(2)–P(4)	23.76
		P(3)–P(4)	18.20

Complex **3** provides a good opportunity to study the relationship between the through metal–metal quadruple bonding coupling $|^3J_{\text{P-Mo-Mo-P}}|$ and the twist angle P–Mo–Mo–P. The assignments of the NMR spectrum for **3** yield three coupling constants, $|^3J_{\text{P(1)-Mo-Mo-P(3)}}| = 18.44$ Hz, $|^3J_{\text{P(2)-Mo-Mo-P(4)}}| = 23.76$ Hz and $|^3J_{\text{P(3)-Mo-Mo-P(4)}}| = 18.20$ Hz, which couple only through metal–metal quadruple bonds. The twist angles of P(1)–Mo–Mo–P(3), P(2)–Mo–Mo–P(4) and P(3)–Mo–Mo–P(4) are 99.5, 162.4 and 85.4° respectively, which suggests that the through metal–metal quadruple bonding coupling $|^3J_{\text{P-Mo-Mo-P}}|$ is dependent on the twist angle of P–Mo–Mo–P, although the variation is not much. Assuming the stereochemical dependence is of Karplus-like form [15], i.e. $^3J_{\text{P-Mo-Mo-P}} = A + B \cos \theta + C \cos 2\theta$ (θ is the twist angle), the values for A , B and C are calculated as 20.99, -0.50 and 2.79 respectively. The maximum and minimum coupling constants are then calculated as 24.28 and 18.18 Hz respectively. The experimental values of the three through metal–metal couplings $|^3J_{\text{P-Mo-Mo-P}}|$, 18 Hz ($\theta = 93.3^\circ$), 18 Hz ($\theta = 89.0^\circ$) and 24 Hz ($\theta = 162.9^\circ$) reported for the complex $\text{Mo}_2\text{Cl}_4(\text{PEt}_3)(\eta^1\text{-tetrphos-2})$ [3], are consistent with the calculated values which are 18.24, 18.19 and 23.77 Hz respectively. We are preparing complexes such as $\text{Mo}_2\text{Cl}_4(\eta^3\text{-dmmm})(\text{L})$ and $\text{Mo}_2\text{Cl}_4(\eta^3\text{-dpmp})(\text{L})$ which may have different twist angles, to verify further the equation mentioned above.

It is noted that the coupling constants of the two phosphorus atoms that form the bridge, i.e. P(1) and P(2), are 51.24 and 52.05 Hz for **2** and **3** respectively, and those of the two phosphorus atoms that form the chelating ring are 7.73 and 8.25 Hz for **2** and **3** respectively. If the observed couplings can be divided into metal, $^2J_{\text{P-Mo-P}}$ or $^3J_{\text{P-Mo-Mo-P}}$, and backbone, $^3J_{\text{P-C-C-P}}$, contributions, where the latter is assumed to be similar to the coupling in the free ligand [16], the magnitudes of the observed coupling constants would require the

contributions from $^2J_{\text{P(2)-Mo-P(3)}}$ and backbone coupling $^3J_{\text{P-C-C-P}}$ to be of the opposite sign, while the contributions from $^3J_{\text{P-Mo-Mo-P}}$ and $^3J_{\text{P-C-C-P}}$ would be of the same sign. Comparison of the $^3J_{\text{P-C-C-P}}$ value of the free etp ligand, 19.7 Hz, with the observed coupling constants of **2** and **3** clarifies this aspect. The $|^2J_{\text{P-Mo-P}}|$ values of the two chelating phosphorus atoms of these two complexes are thus about 28 ± 1 Hz. This is similar to the value reported for the $[\text{Ph}_2\text{P}(\text{CH}_2)_n\text{PR}'\text{R}'']\text{Mo}(\text{CO})_4$ system which is 28 Hz [16]. The results also suggest that the bridging ring makes a larger contribution to the coupling constant than the chelating ring.

5. Supplementary material

Complete tables of anisotropic thermal parameters, bond distances, and bond angles for complexes **3** and **4** (6 pages), and two listings of observed and calculated structures (37 pages) are available from author J.D.C. upon request.

Acknowledgements

We thank the National Science Council of the Republic of China for support.

References

- [1] F.A. Cotton and R.A. Walton, *Multiple Bonds Between Metal Atoms*, Oxford University Press, London, 2nd edn., 1993.
- [2] (a) J.-D. Chen and F.A. Cotton, *Inorg. Chem.*, 30 (1991) 6; (b) J.-D. Chen, F.A. Cotton and B. Hong, *Inorg. Chem.*, 32 (1993) 2343.
- [3] F.A. Cotton and B. Hong, *Inorg. Chem.*, 32 (1993) 2354.
- [4] C.-T. Lee, S.-F. Chuang, C.-T. Chen, J.-D. Chen and C.-D. Hsiao, *Inorg. Chem.*, 35 (1996) 2930.
- [5] J.V. Brenneke and F.A. Cotton, *Inorg. Chem.*, 9 (1970) 346.
- [6] G.M. Sheldrick, *SHELXTL PLUS*, release 4.1, Siemens Analytical X-ray Instruments Inc., Karlsruhe, Germany, 1991.
- [7] P.A. Agaskar and F.A. Cotton, *Inorg. Chem.*, 25 (1986) 15.
- [8] F.A. Cotton and S. Kitagawa, *Inorg. Chem.*, 26 (1987) 3463.
- [9] F.A. Cotton and S. Kitagawa, *Polyhedron*, 7 (1988) 463.
- [10] F.A. Cotton and B. Hong, *Prog. Inorg. Chem.*, 40 (1992) 179.
- [11] R.B. King, *J. Coord. Chem.*, 1 (1971) 67.
- [12] A.L. Bulech, M.M. Olmstead and D.E. Oram, *Inorg. Chem.*, 25 (1986) 298.
- [13] F.A. Cotton and M. Matusz, *Inorg. Chem.*, 26 (1987) 984.
- [14] M. Di Vaira, S. Midollini and L. Sacconi, *Inorg. Chem.*, 18 (1979) 3466.
- [15] M. Karplus, *J. Am. Chem. Soc.*, 85 (1963) 2870.
- [16] S.O. Grim, R.C. Barth, J.D. Mitchell and J.D. Gaudio, *Inorg. Chem.*, 16 (1977) 1776.